CLM - P 333

UKAEA RESEARCH GROUP

Preprint

SPECTROGRAPH CALIBRATION AT SOFT X-RAY WAVELENGTHS

II - From branching ratios to the visible and near U.V.

F E IRONS
N J PEACOCK

CULHAM LABORATORY
Abingdon Berkshire

1973

CLM-P 333

SPECTROGRAPH CALIBRATION AT SOFT X-RAY WAVELENGTHS

II - From branching ratios to the visible and near U.V.

by

F E IRONS* and N J PEACOCK

(Submitted for publication in J. Phys., E., Sci. Instrum.)

ABSTRACT

A grazing incidence spectrograph has been calibrated for absolute intensity at several points in the wavelength range 25 - 33 Å by the method of branching ratios, using line pairs such as C VI (1-7)25.83 Å, (6-7) 3434 Å which are observed in a laser-produced carbon plasma. Experimental results are presented for Ilford Q2 emulsion, used with a two-metre, 600 grooves/mm, gold-coated, catalogue grating, at an angle of incidence of 88°, and agreement is found with a second calibration based on X-ray K-line emission from a standard source.

* Now at the Department of Engineering Physics, Research School of Physical Sciences, Australia National University, Box 4, P.O. Canberra, A.C.T. 2600, Australia.

UKAEA Research Group
Culham Laboratory
Abingdon
Berks.

February 1973

1. INTRODUCTION

The high density, high temperature plasma produced by the laser irradiation of a solid target in vacuum is a rich source of spectral lines. Of present interest are the visible and near u.v. lines from high quantum levels of carbon V and VI reported by Boland et al., (1968a) and listed here in table 1. These will be referred to as the long wavelength lines.

In this paper we wish to report that the resonance lines from the same high quantum levels of carbon V and VI have been resolved with a well-focussed grazing incidence spectrograph, and that both sets of lines, when recorded simultaneously, have been used to calibrate this spectrograph for absolute intensity by the branching ratio method. The resonance lines, which also are listed in table 1,will be referred to as the short wavelength lines.

The calibration reported here arose from a study of recombination in laser-produced plasmas (Irons and Peacock, 1973, hereafter called paper B) for which absolute intensity measurements are necessary. Greater attention has here been paid to the geometry of the plasma viewed by the spectrograph in order to present the calibration in a form which is independent of the plasma. Since the calibration can in principle be extended over a much wider wavelength range than considered here, the present results serve mainly to illustrate the application of a laser-produced plasma as a calibration light source. The results provide however a valuable check on other methods of calibration at soft X-ray wavelengths.

2. THE BRANCHING RATIO METHOD OF INTENSITY CALIBRATION

The branching ratio method of intensity calibration has been described by Griffin and McWhirter (1962) and by Hinnov and Hofmann

(1963). Briefly, it consists of the simultaneous detection of two spectral lines which have a common upper level and which are optically thin. If the intensities of these two lines are denoted by I_{1n} and I_{mn} (ergs s^{-1} cm^{-2} sr^{-1}) we then have

$$\frac{I_{1n}}{I_{mn}} = \frac{A_{1n}}{A_{mn}} \frac{\lambda_{mn}}{\lambda_{1n}} \qquad \ldots (1)$$

where A denotes transition probability, λ denotes wavelength, and the subscripts denote the principal quantum numbers of the upper state (n) and of the lower states (1, m). We identify I_{1n} with the short wavelength lines in table 1, and I_{mn} with the long wavelength lines. On comparing the intensity of the long wavelength lines with some readily-available standard lamp we can derive directly, using equation 1, the absolute intensity of the plasma emission for the lines in the soft X-ray region.

For the successful application of this method of calibration it is essential that the lines are optically thin. This is discussed in section 6. It is also essential that the transition probabilities, A, are accurately known. For C VI, values of A accurate to within 1% were obtained by multiplying those for hydrogen by $Z^4 = 6^4$ (Wiese et al, 1966). For CV, a value $\omega A_{17} = 5.4 \pm 0.5 \times 10^{10}$ s^{-1}, where ω denotes a statistical weight, was calculated on the basis of a linear interpolation of f values (following Smith and Wiese, 1971), and a value $\omega A_{67} = 5.2 \pm 0.3 \times 10^{10}$ s^{-1} was calculated by the method of Bates and Damgaard (1949).

It should also be noted that, for C VI, all substates of the upper level contribute to the long wavelength line, but only the P substate contributes to the short wavelength line. Likewise for CV,

all substates of the upper level (excluding ^1S, ^3S, ^1P, ^3P - see Irons, 1973) contribute to the long wavelength line, but only the ^1P substate contributes to the short wavelength line. Consequently it is necessary to have some knowledge of the distribution of electrons amongst substates before the method of branching ratios can be applied. For the present transitions it can be shown (e.g. by substituting in the formula of Hinnov and Hofmann, 1963) that the lifetime against collision-induced transitions amongst substates ($\sim 10^{-14}$ s) is much smaller than the radiative lifetime of the P substate ($\sim 10^{-11}$ s). It is therefore valid to assume a statistical distribution of substates, which at the values of electron temperature of interest here ($k T_e \gtrsim 30$ eV), means a distribution proportional to statistical weights.

3. GRAZING INCIDENCE SPECTROGRAPH

The grazing incidence spectrograph was of the type described by Gabriel et al (1965) and manufactured by Hilger and Watts. It was operated at an 88^o angle of incidence, with a Bausch and Lomb, two-metre, 600 g/mm gold-coated grating, with a listed blaze angle of $1^o 31'$ (catalogue no. 35-52.40.400 serial no. 2278-27). The entrance slit assembly was redesigned to have the slit jaws on the side of the assembly away from the grating. This enabled the plasma to be formed closer to the slit jaws (section 4). Spatial resolution was achieved by inserting a suitable aperture in the optical path of the spectrograph, between the entrance slit and the grating.

The spectrum was recorded on Ilford Q2 photographic plates, developed in 1D 19 for the recommended time ($3\frac{1}{2}$ minutes at 20^oC) and fixed in Amfix for 2 mins. At the wavelengths of interest here the photographic density has been shown to be linear with intensity

up to a density of 0.2 (Morgan et al, 1968). During the course of the experiment we verified this fact with data from the laser-produced plasma itself. The spatial distribution of the spectra at right angles to the direction of wavelength dispersion provides a continuous variation of density; while the division in the intensity between first and second orders is a constant for a given wavelength, being dependent only on the diffraction efficiencies between the orders. This method is mentioned because it should be useful for measuring plate response over a wide range of wavelengths. The densities involved in the present work do not exceed 0.2.

The linearity of density with the number of superimposed shots was verified by recording seven spectra, for which the number of superimposed shots varied from 5 to 45. In the subsequent plot of density versus number of shots only one data point deviated more than 30% from the straight line of best fit.

4. EXPERIMENTAL ARRANGEMENT

In addition to the grazing incidence spectrograph, a 1.5 m focal length Ebert monochromator has been used to record the long wavelength radiation from the plasma. A quartz-lithium fluoride achromat was used to focus this radiation onto the entrance slit of the monochromator. The signal at the exit slit was monitored by a quartz-window (EMI 9594 QB) photomultiplier operated within its linear response range and displayed on a Tektronix 519 oscilloscope, the total rise time of the system being $\sim$ 3 ns. Absolute intensity calibration of the monochromator and associated optics was achieved by means of a tungsten strip lamp.

The grazing incidence spectrograph and the monochromator were set up to view the plasma from almost opposite directions, as shown in fig.1. The monochromator was offset a few degrees to avoid

reflections from the spectrograph slit jaws, which also were covered with tape to eliminate reflection. Measurements with the two instruments were made simultaneously.

The plasma light source was produced by irradiating a polyethylene $(C_2H_4)_n$ target with a pulsed neodymium glass laser beam which is focussed in vacuo ($< 10^{-4}$ torr) through a 10 cm focal length lens at near normal incidence on to the target surface. The laser was switched in the "pulse transmission mode" to give 6J of energy in a pulse of duration 6 nsec, rising to peak intensity in 1.5 nsec. The target was in the form of a disc which could be rotated between shots. The laser power was chosen sufficiently high to ionise the carbon plasma to the ion stage C^{6+}.

The plasma expands away from the point of laser focus on the target, preferentially about an axis, hereafter referred to as the plasma axis, which is inclined at a few degrees to the target normal. The plasma axis is parallel (within a few degrees) to the entrance slit of the grazing incidence spectrograph and is at the centre of the angle of acceptance of the spectrograph. The distance of the plasma axis from the entrance slit (4 mm) is smaller than the minimum distance needed for optimum light collection, but has the advantage that the instrumental aperture (F/60) determines the dimension of plasma seen by the spectrograph (0.067 mm) in a direction normal to the plasma axis. This eliminates the need for a precise measurement of the actual physical dimension of the plasma in this direction. Nevertheless a somewhat less-than-precise measurement was necessary to establish the above fact, and the spatial distribution thus measured (by scanning the long wavelength radiation with the Ebert

monochromator) is shown in figure 1, indicating a dimension of $\sim$ 1.5 mm at a distance of 1 mm from the target. Full details of a similar spatial distribution and its variation with time may be found in Irons et al (1972). In a direction parallel to the plasma axis there is a significant variation of intensity over the region (0.5 mm) of spatial resolution determined by the aperture in the grazing incidence spectrograph, and here a precise scan by the Ebert monochromator has been necessary.

4.1 SPECTRAL LINE DETECTION

For the short wavelength lines, adequate spectral resolution was achieved with good intensity on the plate with an entrance slit width of 10 μ, a spatial resolution of 0.5 mm and a 34 shot exposure. The spatial resolution of 0.5 mm was insufficient only within 1 mm of the target and here an estimate of the true intensity distribution was made (following Boland et al, 1968a) and is illustrated in the insert to figure 2. The necessary correction to the observed intensity (25% at 0.5 mm and 15% at 1.0 mm) has been included in the results to follow. Because line intensity decreases rapidly with distance from the target there is a maximum distance at which the short wavelength lines can be detected ($\sim$ 1.6 mm under the above conditions).

For the long wavelength lines, detection is possible well beyond 10 mm from the target. However these lines show strong Stark broadening, especially close to the target where the density is highest (Irons, 1973). There is a minimum distance ($\sim$ 1 mm) at which these lines can be detected above the background continuum, which also is strongest close to the target. Details of the region of overlap where both lines in a branching pair can be detected are shown in

table 1, and the results to follow represent averages over this region.

The restrictions on detectability which have been described above become progressively relaxed for lower members of the line series. For example, the line pair C VI (1-6) 26.03 Å, (5-6) 2070 Å can be detected together over the distance 0.5 - 5.0 mm from the target. The ratio of intensities of these two lines over this distance range is shown in figure 2 and will be used later in our consideration of opacity (section 6.2).

5. SPECTROGRAPH SENSITIVITY

In common with Morgan et al (1968) we define a spectrograph sensitivity S_λ at the wavelength λ in the first order spectrum as

$$S_\lambda = W\, G_\lambda\, P_\lambda$$

where W is the entrance slit width, G_λ is the grating efficiency and P_λ is the plate response factor. In their paper, Morgan et al showed that if $\int F_\lambda \, d\lambda$ (ergs s^{-1} sr^{-1}) is the total intensity of a line emitted by a source which is within the acceptance angle of the spectrograph and if $\int D_\lambda \, dx$ is the integrated microdensitometer image of the line on the photographic plate, then

$$S_\lambda = \frac{r_1\, r_2 \int D_\lambda \, dx}{t \int F_\lambda \, d\lambda} \qquad \ldots (2)$$

where t is the exposure time, and r_1 and r_2 are the distances from the source to the entrance slit and to the photographic image respectively.

Morgan et al, working with a steady state X-ray source, were able to measure $\int F_\lambda \, d\lambda$ in a supplementary experiment, by means of a flow proportional counter with photon counting. For the present

application, we note that

$$t \int F_\lambda \, d\lambda = \iint I_{1n} \, dt \, dA$$

where the intensity of the short wavelength line is integrated in time and over the area of plasma seen by the spectrograph. From the branching ratio equation, (1), it follows that

$$t \int F_\lambda \, d\lambda = \frac{A_{1n}}{A_{mn}} \frac{\lambda_{mn}}{\lambda_{1n}} \iint I_{mn} \, dt \, dA \, . \qquad \ldots (3)$$

The integration of the intensity of the long wavelength line is readily achieved with the data from the Ebert monochromator.

Substitution of the measured values of $\int D_\lambda \, dx$ and $t \int F_\lambda \, d\lambda$ (from equation (3)) into equation (2), along with $r_1 = 0.4$ cm and $r_2 = 20$ cm for CV1 (and slightly more for CV), gives the values of S_λ shown in table 1.

TABLE 1

Spectrograph Sensitivity S_λ.

Branching line pairs	Long wave-length (Å)	Short wave-length (Å)	Region of overlap	$S_\lambda \times 10^4$ density $erg^{-1}\ cm^3$
CVI 1 - 7		25.83		
6 - 7	3434		1.0-1.6 mm	0.8 ± 0.3
CVI 1 - 8		25.70		
7 - 8	5290		∿1.6 mm	0.9 ± 0.3
CVI $\varepsilon(\lambda_1)$		25.33		
6 - 7	3434		1.0-1.6 mm	1.1 ± 0.3
CV 1 - 7		32.19		
6 - 7	4945		∿1.6 mm	0.9 ± 0.4
X-ray source calibration		O_{K_α} (23.6 Å)		1.1 + 0.4

An interesting variation of the above method is to choose the C VI Lyman free-bound continuum at, say, the continuum edge λ_1 as the short wavelength transition, and the line C VI (6-7) as the long wavelength transition. The concept of a common upper level is no longer relevant. However the quantum level C VI n = 7 is above the thermal limit (paper B) and the intensity of the line C VI (6-7) can be expressed in terms of the Saha-Boltzmann equation of local thermal equilibrium (L.T.E.). Expressions for the continuum intensity $\varepsilon(\lambda)$ (ergs $s^{-1}\ cm^{-2}\ sr^{-1}\ Å^{-1}$) and the line intensity I_{67} are given e.g. by Boland et al (1968a). From these it can be shown that

$$t\,F_\lambda = \iint \varepsilon(\lambda_1)\,dt\,dA = 1.50 \times 10^3\, e^{-\frac{X_7}{k\,T_e}} \iint I_{67}\,dt\,dA \quad \ldots (4)$$

where X_7 denotes the ionisation potential from the level n = 7. The value of T_e necessary to evaluate equation (4) can be deduced from the free-bound continuum intensity (paper B).

Substitution of equation (4) into an equation similar to (2) along with measured values of D_λ, $\frac{dx}{d\lambda}$ and I_{67} gives the value of S_λ shown in table 1.

The advantages of using a continuum transition for this calibration are that the densitometry becomes more straightforward and the need for good spectral resolution is relaxed. From the latter it follows that a wider entrance slit can be used, with a consequent gain in light intensity. Also, as pointed out later (section 6) the continuum is less likely to be affected by opacity than the resonance lines.

The r.m.s. error in S_λ is approximately $\pm$ 35%. This is composed of errors in the tungsten lamp calibration ($\pm$ 12%), in the detection of the long wavelength lines above the continuum ($\pm$ 20%), in the integration of I_{1n} over the volume of plasma seen by the spectrograph ($\pm$ 15%), in the measurement of density from the photographic plate ($\pm$ 20% - includes plate-to-plate variability as determined over 7 plates), in the use of the formula (equation 2) for S_λ for small r_1 (< 1%), and in the ratio of transition probabilities (< 1% for CVl and < 5% for CV).

Errors due to opacity effects which are not included above but are considered separately in section 6 are expected to be < 20%.

5.1 CALIBRATION WITH THE X-RAY SOURCE

A method of intensity calibration which uses an X-ray source of discrete K lines whose intensities are monitored by a flow proportional counter has been described by Morgan et al (1968), and employed by Boland et al (1968b) and Jones and Freeman (1968). The source of Jones and Freeman was used by us to calibrate our spectrograph, at the wavelength (23.6 $\mathring{A}$) of the oxygen K_α line, following the procedure described by Morgan et al. The resultant calibration, which is included at the foot of Table 1, is in good agreement with the branching ratio calibration. Evidently, at the wavelengths of interest here, there is no reciprocity failure between the $\sim 10^{-8}$s exposure of the laser produced plasma and the $\sim 10^{3}$s exposure of the X-ray source. A similar result has been obtained by Birks et al (1970).

In the preceding paper (Hobby & Peacock, 1973), the spectrograph sensitivity is constructed from separate measurements of the grating efficiency G_λ (Speer, 1972) and of the plate response factor P_λ using a K_α, X-ray source. The good general agreement between the sensitivities quoted in this and the preceding paper indicates that P_λ at X-ray wavelengths is independent of exposure time when the latter is varied over ten orders of magnitude.

6. OPACITY

Implicit in the interpretation of intensities so far has been the assumption of optical transparency. Theoretical and experimental evidence for this assumption is now considered.

6.1. THEORETICAL CONSIDERATIONS OF OPACITY.

We have the following criterion that the intensity of a spectral

line does not depart from its optically thin value by more than 10% (Cooper, 1966).

$$N_1 \; D \; f_{1n}\left(\frac{\pi e^2}{mc}\right) \quad \left\{1 - \frac{\omega_1 \; N_n}{\omega_n \; N_1}\right\} \quad \phi_o \lesssim \begin{cases} 0.28 & \text{Doppler} \\ 0.40 & \text{dispersion} \end{cases} \quad \ldots \; (5)$$

where D(cm) is the plasma dimension, f_{1n} is the absorption oscillator strength, $N(cm^{-3})$ and ω denote number density and statistical weight respectively, and the subscripts refer to the upper state, n, and to the lower state 1(or m). Two profile shapes are considered in equation (5), namely thermal Doppler and dispersion, for which $\phi_o = (\frac{\ln 2}{\pi})^{\frac{1}{2}} \; \frac{1}{\nu_{\frac{1}{2}}}$ and $= \frac{1}{\pi \; \nu_{\frac{1}{2}}}$ respectively, where $\nu_{\frac{1}{2}}$ is the half half-width in frequency units (s^{-1}).

The long wavelength lines all show strong Stark broadening (Irons, 1973) and can be approximated with a dispersion profile. Substituting values of $\nu_{\frac{1}{2}}$, typical of the region 1.0 - 1.6 mm into equation (5) gives values $N_1 \; D$ (neglecting for the moment the stimulated emission term $\{1 - \frac{\omega_1 \; N_n}{\omega_n \; N_1}\}$), from which we can calculate lower (Boltzmann) limits to $N_n D$ and thence lower limits to the intensities of the long wavelength lines corresponding to 10% self-absorption. These intensities are an order of magnitude greater than those observed, indicating that opacity is not an important effect. Indeed this difference becomes two orders of magnitude when we include a factor $\{1 - \frac{\omega_1 \; N_n}{\omega_n \; N_1}\} \simeq 1 - e^{-h\nu/KT}$ for the stimulated emission term (the high quantum levels being near Boltzmann equilibrium, paper B). An alternative way of expressing the latter result is to say that the densities required for 10% self-absorption in the long wavelength lines are an order of magnitude greater than those observed here.

The wavelength profiles of the short wavelength lines are Doppler, rather than Stark broadened (the magnitude of the Stark broadening was calculated from Griem (1960) with suitable Z scaling for the perturbing ion). Structure within the Doppler profile is due to both streaming and random ion motion. The streaming motion produces a systematic distribution of velocities along the line of sight with no opportunity for absorption. An estimate of the random component and of the depth of plasma over which absorption is possible was made from the work of Irons et al (1972), allowance being made for the fact that the expansion velocities observed here are $\sim$ 30% smaller than those reported in the earlier publication. Substituting into equation (5) and noting that the stimulated emission term is here unity, we find $N(C^{5+}) \lesssim 3 \times 10^{18}$ cm^{-3} as the condition for transparency of CVI and $N(C^{4+}) \lesssim 8 \times 10^{17}$ cm^{-3} as the condition for transparency of CV. Measurement (see section 6.2) gives $N(C^{5+}) \gtrsim 4 \times 10^{17}$ cm^{-3}; and we may assume a comparable value for $N(C^{4+})$(see eg. Boland et al, 1968 a); in which case the above inequalities are satisfied and the plasma may be considered optically thin to the short wavelength lines. The above procedure is only an approximation, but a full scale study of radiative transfer for the conditions of a laser-produced plasma, which clearly is needed, is beyond the scope of this paper. However, the above inequalities for $N(C^{5+})$ and $N(C^{4+})$ are not likely to be in error by more than a factor of five.

Nevertheless we are less justified in assuming the short wavelength lines to be optically thin than the high wavelength lines and this is one reason for considering the C VI free-bound continuum as

an alternative short wavelength transition.

We have the following criterion that the intensity of the Lyman free-bound continuum of a hydrogenic ion of charge Z does not depart from its optically thin value by more than 10% (Cooper, 1966) where stimulated recombinations are neglected

$$D\, N_1 \lesssim 2.6 \times 10^{16}\, Z^2 \quad . \qquad \ldots (6)$$

The expression in equation (6) has been evaluated at the continuum edge, which is the wavelength of interest here, and where also the absorption is a maximum. With Z = 6 and D = 0.15 cm equation (6) becomes $N_1 = N(C^{5+}) \lesssim 6 \times 10^{18}$ cm^{-3} which is well satisfied by the measured value $N(C^{5+}) \approx 4 \times 10^{17}$ cm^{-3}.

6.2 EXPERIMENTAL CONSIDERATIONS OF OPACITY

In paper B the intensities of the short wavelength lines have been analysed in conjunction with the intensity of the free-bound continuum and the results are consistent with these lines being optically thin and with their upper states being in L.T.E. with the free electrons. This later fact justifies the use of the Saha-Boltzmann equation to interpret the absolute intensities of the long wavelength lines to give ion densities (paper B). The densities so deduced are in factor-of-two agreement with densities derived from Stark broadening and from interferometry in similar laser produced carbon plasmas,(Aglitzky et al, 1971; Basov et al, 1971; and Irons, 1973). This then constitutes evidence that the long wavelength lines are not seriously affected by opacity, and justifies the use (in section 6.1) of densities deduced from line intensities.

The experimental procedure which has been adopted to detect

opacity effects (e.g. Griffin and McWhirter, 1962) is to study the line intensity ratio $\frac{I_{ln}}{I_{mn}}$ as a function of density. In the present case of a plasma produced from a solid target this has been achieved by varying the point of observation to different distances from the target and making use of the fact that density is a rapidly decreasing function of distance.

The line pairs in table 1 can only be observed together over a limited region of space. It is more rewarding to consider the line pair CVI (1-6), (5-6) which, as explained in section 4.1, can be observed over the region 0.5 - 5.0 mm (figure 2). Included in figure 2, on the abscissa, is the product N_e (electron density) x plasma depth which is related to the opacity. Within experimental limits there is no significant variation of the intensity ratio of these lines over more than an order of magnitude of the product N_e x plasma depth. Since the likelihood of the lines in table 1 being affected by opacity is less than that of the lines C VI (1-6), (5-6) (this follows from equation (5)) we are therefore justified in asserting that opacity is not an important effect in the plasma region of interest for any of the lines in table 1.

7. DISCUSSION

A laser-produced plasma has been shown to be a suitable light source for the branching ratio method of intensity calibration. This conclusion has been reached only after paying attention to experimental detail involving a compromise between spectral resolution, spatial resolution and number of shots (section 4.1).The effect of high density on opacity is offset by the small physical dimension. For the spatial region of interest (1.0 - 1.6 mm from the target) theory indicates that the lines should be optically thin, and this is

supported by experiment (section 6). The good agreement between the various C VI branching ratios and between these and the X-ray source calibration (table 1) also indicates that opacity in this region of the plasma is not a problem.

Experimental results have been presented for the element carbon and in particular for transitions which fall in the wavelength range 25-33 Å, which is the particular wavelength range of interest in the associated experiment (paper B). In principle, however, the calibration can be extended to other wavelengths in the range 10-100 Å by a choice of other second sequence elements as target material, and indeed to wavelengths > 100 Å by a choice of transitions onto the first and higher excited states as the short wavelength transition. At wavelengths > 100 Å, reciprocity effects may affect the emulsion response and it may prove useful to extend the duration of the CVI light pulse by allowing two laser-produced plasma plumes to collide (Basov et al., 1968).

The calibration described here represents an extension of the branching ratio method of calibration in the sense that the line pairs reported here branch directly from the soft X-ray to the visible and near u.v. regions of the spectrum. The agreement between this calibration and the calibration based on an X-ray source of oxygen K_α of known intensity (see table 1) provides a useful check on this latter method of calibration. Good general agreement has also been obtained with a calibration based on measurements of the absolute efficiency of the diffraction grating (Hobby and Peacock, 1973).

8. CONCLUSION

The paper has described the application of a laser-produced plasma as a light source for the branching ratio method of intensity calibration. The calibration presented here, for the wavelength range 25-33 Å, can in principle be extended over a much wider wavelength range by using elements other than carbon as the target material and transitions other than those which terminate on the ground state as the short wavelength transition.

9. ACKNOWLEDGEMENTS

We are grateful to Mr A W Waller (A.W.R.E. Aldermaston) for supplying the redesigned entrance slit assembly for the spectrograph, and to Mr B B Jones and Mr F F Freeman (of the Astrophysics Research Unit, S.R.C.) for permission to use their X-ray source and for valuable advice on its operation. We would like to thank Mr A H Jones for his assistance with the construction of the laser, for its day-to-day operation, and for his general assistance with the experiment. We are also grateful to Dr R W P McWhirter (of the Astrophysics Research Unit, S.R.C.) for his criticism of the manuscript.

REFERENCES

AGLITZKY, E.V., BASOV, N.G., BOIKO, V.A., GRIBKOV, V.A., ZAKHAROV, S.A., KROKHIN, O.N., and SKLIZKOV, G.V., 1971, Tenth International Conference on Phenomena in Ionised Gases, Oxford p.229.

BASOV, N.G., KROKHIN, O.N., and SKLIZKOV, G.V., 1968,I.E.E. J.Qu.Elect., 12, 988-91.

BASOV, N.G., BOIKO, V.A., GRIBKOV, V.A., ZAKHAROV, S.M., KROKHIN, O.N., and SKLIZKOV, G.V., 1971, Zh. Eksp. Teor. Fiz. 61, 154-61 [J.E.T.P. 34, 81-4, 1972].

BATES, D.R., and DAMGAARD, A., 1949, Phil. Trans. R. Soc. 242A, 101-22.

BIRKS, L.S., WHITLOCK, R.R., VIERLING, J.S., NAGEL, D.J., and GORBICS, S.G., 1970, J.O.S.A. 60, 649-53.

BOLAND, B.C., IRONS, F.E., and McWHIRTER, R.W.P. 1968a, J.PHYS. B: Atom. Molec. Phys. 1, 1180 - 91.

BOLAND, B.C., JONES, T.J.L., and McWHIRTER, R.W.P., 1968b, Conf. on Calibration Methods in the Ultraviolet and X-ray Regions of the Spectrum, Munich; E.S.R.O. Report SP-33, 59-65.

COOPER, J., 1966. Reports on Progress in Physics, 29, 35-130.

GABRIEL, A.H., SWAIN, J.R., and WALLER, W.A., 1965, J. Sci. Instrum., 42, 94-7.

GRIEM, H.R., 1960, Astroph. J. 132, 883-93.

GRIFFIN, W.G., and McWHIRTER, R.W.P., 1962, Proc. Conf. on Optical Instruments and Techniques Ed. K.J. Habell (London: Chapman and Hall), pp.14-21.

HINNOV, E., and HOFMANN, F.W., 1963,J.O.S.A. 53, 1259-65.

HOBBY, M.,and PEACOCK, N.J.,1973,to be published (preceding paper).

IRONS, F.E., McWHIRTER, R.W.P., and PEACOCK, N.J., 1972,J. Phys. B: Atom. Molec. Phys. 5, 1975-87.

IRONS, F.E., 1973 accepted for publication in J.Phys.B.

IRONS, F.E., and PEACOCK, N.J., 1973, to be published.

JONES, B.B., and FREEMAN, F.F., 1968, Conf. on Calibration Methods in the Ultraviolet and X-ray Regions of the Spectrum, Munich, E.S.R.O. Report SP-33, 245-52.

MORGAN, F.J., GABRIEL, A.H., and BARTON, M.J., 1968,J. Phys. E. 1, 998-1002.

SMITH, M.W., and WIESE, W.L. 1971, Astrop. J. Suppl. No. 196, 23, 103-192.

SPEER, R.J., 1972. "Atoms and Molecules in Astrophysics", paper 8, p.285-310, published by Academic Press.

WIESE, W.L., SMITH, M.W. and GLENNON, B.M., 1966 National Standard Reference Data Series, Report NSRDS-NBS4 Washington 1, 1-152.

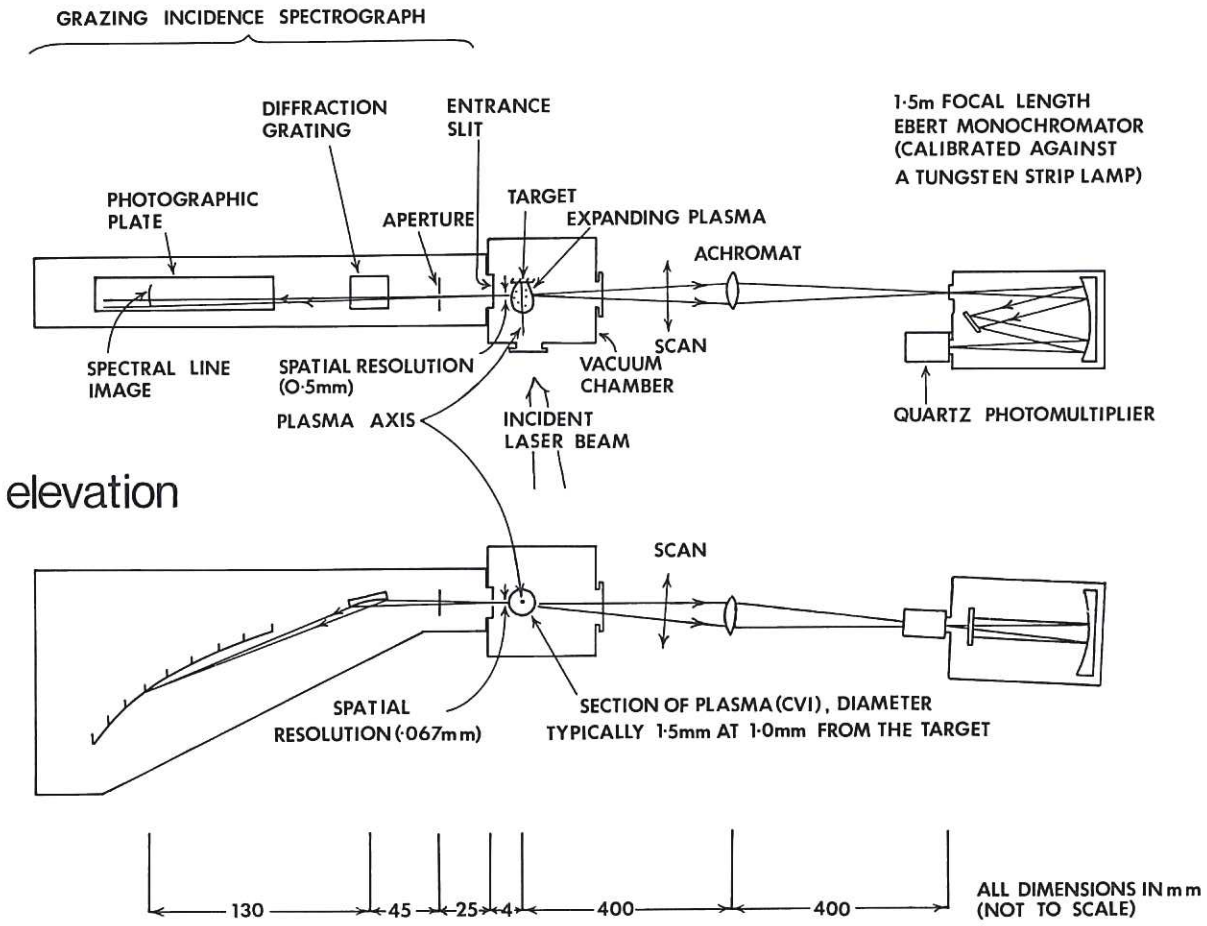

Fig. 1 Sections of the apparatus, in the plane of the target normal (plan view) and in a vertical plane at right angles to the target normal (elevation view), showing (left to right) the grazing incidence spectrograph, the laser-produced plasma and the Ebert monochromator.

CLM - P 333

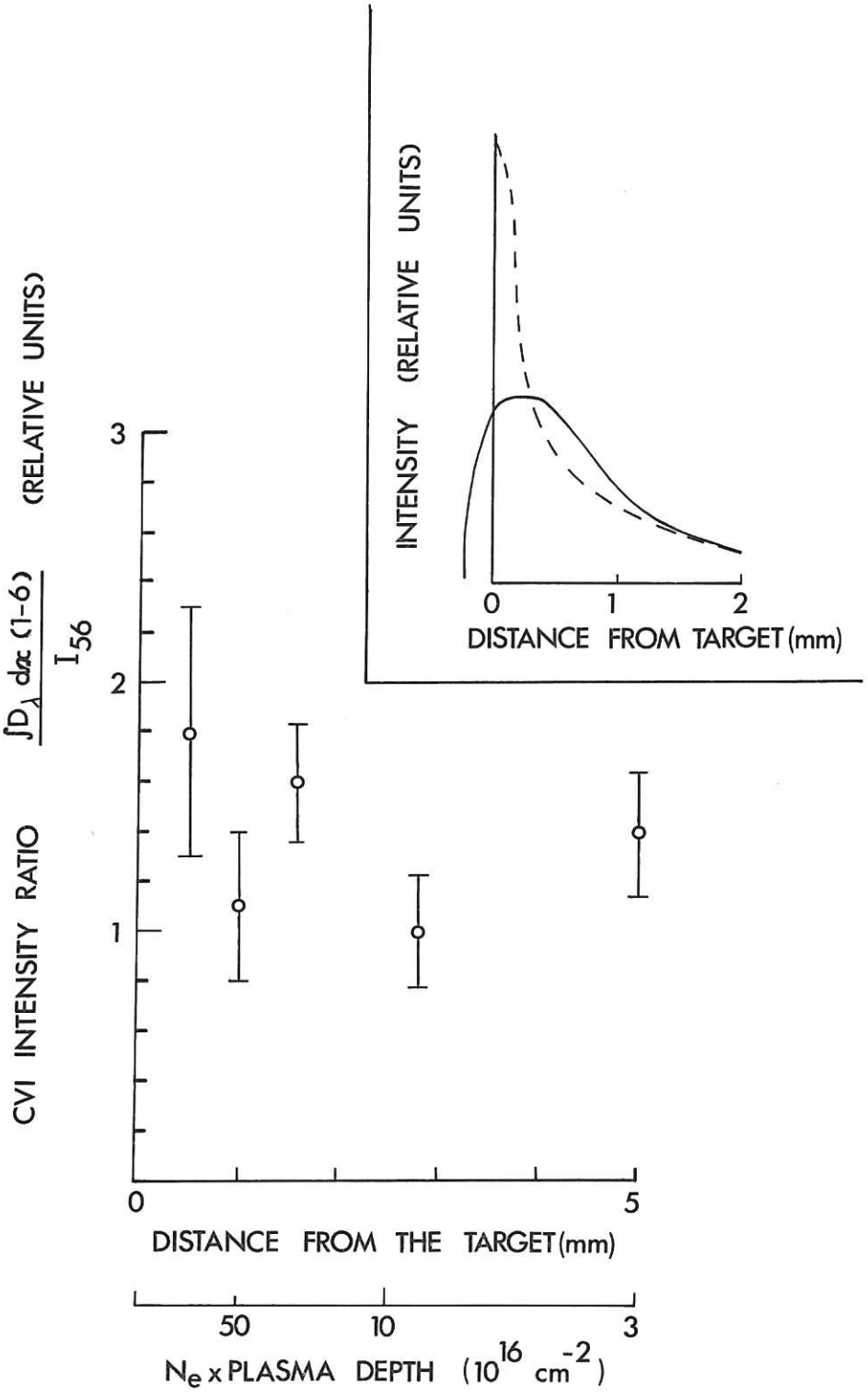

Fig. 2 The figure shows the ratio of the density of the CVI (1-6 line), $\int D_\lambda \, dx$, to the intensity, I_{56} of CVI as a function of distance from the target. The grazing-incidence spectrograph is used to record the resonance transition, CVI (1-6), on emulsion within the linear range of the photographic density. The points at 0.5 mm and 1 mm have been reduced by 25% and 10% respectively to compensate for the limited spatial resolution as illustrated in the insert. The insert shows how the true intensity distribution (– – –) of CVI (1-6) is smoothed out by the limited spatial resolution of 0.5 mm to give the measured intensity distribution (————).

CLM-P333